6.9. Stokes-correlometry of polarization-inhomogeneous objects

A.G. Ushenko, A.V. Dubolazov, G.B. Bodnar,
V.T. Bachinskyi, O. Vanchuliak

6.9.1. Theoretical basics and experimental realization of the method of stokes-correlometry of biological layers

6.9.1.1. Brief theory

In the series of research works the possibility of polarimetry diagnostic [1-19] of optically anisotropic biological layers is demonstrated. Separate place in such investigations occupy laser polarimetry of optically thin (non-depolarizing) layers of biological tissues [20-22] and fluids [23-34]. At that high sensitivity of laser polarimetry techniques is achieved [9,11,13,16,17]. It is determined by the significant range of differences in average (within the test groups of biological layers and those under study) values of statistical points that characterize the distribution of polarization parameters (polarization azimuth and ellipticity) of the series of microscopice images [5,8-11,15,16,22,24,28]. To describe the correlation structure of the stationary distributions of the fields of complex amplitudes of laser light converted by optically anisotropic biological layers, one can use the following mutual spectral density matrix [35]

$$W_{i,j}(r_1, r_2) = E_i^*(r_1) \cdot E_j(r_2), i, j = x, y \tag{6.9.1}$$

Here r_1 and r_2 - the coordinates of the neighboring points in the field of laser radiation.

In this work we have to analyze the 4th (the degree of crystalization) Stokes vector parameter.

Using this matrix operator one can introduce the following expression for the "two-point" Stokes vector parameters

$$S_4 = i\left[W_{yx}(r_1, r_2) + W_{xy}(r_1, r_2)\right] = i\left[E_x^*(r_1)E_y(r_2) + E_y^*(r_1)E_x(r_2)\right]. \qquad (6.9.2)$$

Using relations (6.9.2) the following algorithms to calculate the "two-point" Stokes vector parameters (hereinafter "Stokes-correlometry parameters" - SCP) can be obtained

$$S_4 = \left[E_{y1}E_{x2}\sin\delta_1 + E_{y2}E_{x1}\sin\delta_2\right] + i(E_{x2}E_{y1}\cos\delta_1 + E_{x1}E_{y2}\cos\delta_2). \qquad (6.9.3)$$

In order to simplify the physical analysis of manifestations of optical anisotropy (distributions of optical axes directions $\rho(r) = arctg\dfrac{E_y(r)}{E_x(r)}$ and phase shifts $\delta(r)$ between the orthogonal components ($E_x(r), E_y(r)$) of laser wave amplitude) of biological layers

$$\begin{cases} S_4 = \mathrm{Re}\,S_4 + \mathrm{Im}\,S_4 = \left(\sin\delta_1 + ctg\rho_2 tg\rho_1 \sin\delta_2\right) + i\left(\cos\delta_1 + ctg\rho_2 tg\rho_1 \cos\delta_2\right); \\ |S_4| = \sqrt{\left[1 + ctg^2\rho_2 tg^2\rho_1 + 2ctg\rho_2 tg\rho_1 \cos(\delta_2 - \delta_1)\right]}; \\ ArgS_4 = arctg\left(\dfrac{\cos\delta_1 + ctg\rho_2 tg\rho_1 \cos\delta_2}{\sin\delta_1 + ctg\rho_2 tg\rho_1 \sin\delta_2}\right). \end{cases} \qquad (6.9.4)$$

In the approximation of weak phase fluctuation relation (6.9.4) has the form of

$$\begin{cases} |S_4| = 1 + ctg\rho_2 tg\rho_1; \\ ArgS_4 = arctg\left(\dfrac{1 + ctg\rho_2 tg\rho_1}{\delta_1 + \delta_2 ctg\rho_2 tg\rho_1} \right). \end{cases} \quad (6.9.5)$$

6.9.1.2. Experimental results of the method of Stokes-correlometry

Measurement of the coordinate distributions values is carried out in the experimental arrangement of Stokes-polarimeter [16,31-34].

The modulus $|(S_{i=4}(\Delta x, \Delta y))|$ of the were calculated by the following ratios

$$\left\{ |S_4| = \sqrt{\left[\sqrt{I_0(r_2)I_{90}(r_1)}\sin\delta_1 + \sqrt{I_0(r_1)I_{90}(r_2)}\sin\delta_2\right]^2 + \left[\sqrt{I_0(r_2)I_{90}(r_1)}\cos\delta_2 + \sqrt{I_0(r_1)I_{90}(r_2)}\cos\delta_1\right]^2} \right. \quad (6.9.6)$$

$Arg(S_{i=4}(\Delta x; \Delta y))$ were calculated by the following ratios

$$\left\{ ArgS_4 = arctg\left(\frac{\left[\sqrt{I_0(r_2)I_{90}(r_1)}\cos\delta_2 + \sqrt{I_0(r_1)I_{90}(r_2)}\cos\delta_1\right]}{\left[\sqrt{I_0(r_2)I_{90}(r_1)}\sin\delta_1 + \sqrt{I_0(r_1)I_{90}(r_2)}\sin\delta_2\right]} \right). \quad (6.9.7)$$

Here I_0 and I_{90} - the intensities at the orientation of transmission plane of polarizer 0^0 and 90^0; δ_i - phase shifts between the orthogonal components of the amplitude of the laser radiation in the points with coordinates r_1 and r_2.The results of experimental approbation of the Stokes-correlometry method of optically-thin layer of muscular tissue are illustrated by a series of dependencies (maps and histograms of m_{ik} distributions), which are shown in Fig. 6.9.1.

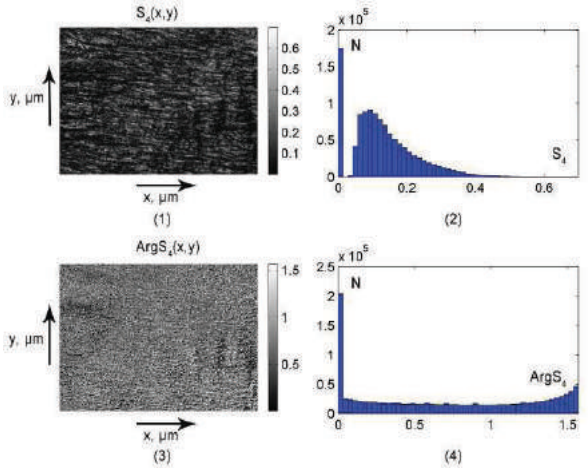

Fig. 6.9.1. Maps (fragments (1),(3)) and histograms (fragments (2, 4) of the distributions of the values of MSV and PhSV of the histological section of skeletal muscle.

Table 6.9.1 presents the results of statistic analysis (statistical moments of the 1st-4th orders $Z_{i=1;2;3;4}$) of coordinate distributions of $|j_{ik}|$ of coordinate distributions of MSV and PhSV of images of skeletal muscle.

Table 6.9.1. Statistical moments $Z_{i=1;2;3;4}$ of the distributions of the values of MSV and PhSV of skeletal muscle

$Z_{i=1;2;3;4}$	$\|S_4\|$	$ArgS_4$
$Z_{i=1}$	0.27	0.89
$Z_{i=2}$	0.34	1.21
$Z_{i=3}$	0.15	0.47
$Z_{i=4}$	0.26	0.82

It was defined the individual sensitivity of the value of $Z_{i=1;2;3;4}$ to the peculiarities of coordinate distributions of MSV $|S_4|$ и PhSV $ArgS_4$. Such a fact was chosen as the basic for applied biomedical usage of statistic analysis of coordinate distributions of MSV $|S_4|$ и PhSV $ArgS_4$.

6.9.2. Clinical application of stokes-correlometry of uterus wall tissue in differential diagnostics of prolapse

6.9.2.1. Objects of investigation

It was investigated two groups of samples of biopsy of uterus wall tissue:

- healthy donors – control group 1 (30 samples);
- affected by prolapse - group 2 (30 samples).

Histological sections were produced due to the standard technique on the freezing microtome.

6.9.2.2. Experimental results

The set of Figs. 6.9.2, 6.9.3 presents the results of Stokes-correlometry mapping of the histological sections of the uterus wall of healthy donors (Fig.6.9.2) and affected by prolapse (Fig. 6.9.3).

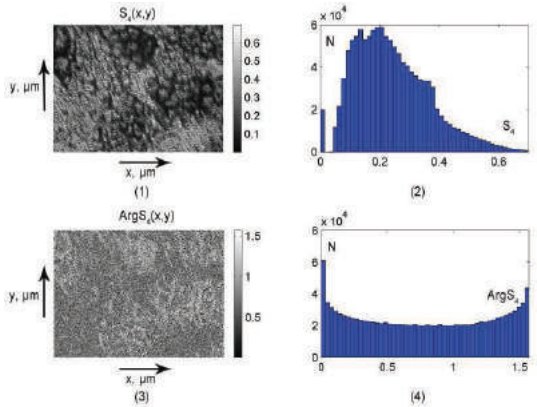

Fig. 6.9.2. Maps (fragments (1),(3)) and histograms (fragments (2, 4)) of the distributions of MSV for healthy donors (fragments (1),(2)) and with prolapse (fragments (3),(4)).

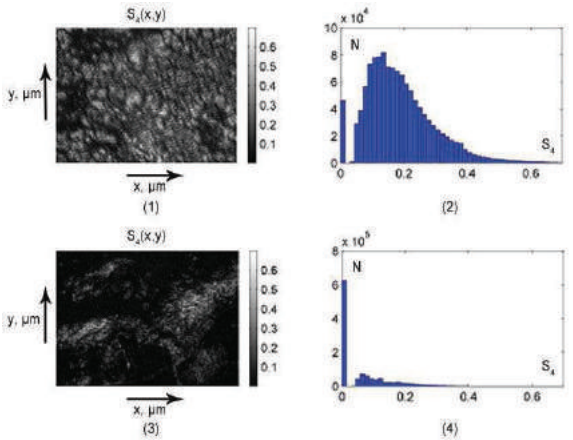

Fig. 6.9.3. Maps (fragments (1),(3)) and histograms (fragments (2, 4)) of the distributions of PhSV for healthy donors (fragments (1),(2)) and with prolapse (fragments (3),(4)).

For the possible clinical application of the Mueller matrix mapping method for each group of samples the operating characteristics, typical for evidence-based medicine [36-38] that determine the diagnostic power of the method are determined, namely – sensitivity ($Se = \frac{a}{a+b}100\%$), specificity ($Sp = \frac{c}{c+d}100\%$) and balanced accuracy ($Ac = \frac{Se+Sp}{2}$), where a and b – the number of correct and incorrect diagnoses within group 2; c and d – the same within group 1 – Table 6.9.2.

Table 6.9.2. Balanced accuracy of Stokes-correlometry

Ac,%	$\lvert S_4 \rvert$	$ArgS_4$
$Z_{i=1}$	91%	77%
$Z_{i=2}$	93%	79%
$Z_{i=3}$	96%	82%
$Z_{i=4}$	93%	85%

It was reached a good ($Ac(ArgS_4) = 82\% - 85\%$) and excellent ($Ac(\lvert S_4 \rvert) = 93\% - 96\%$) level of balanced accuracy of the method of differential diagnostics of healthy donors and with prolapse.

6.9.3. Conclusions

Short theoretical basics of the method of polarization-interference Stokes-correlometry mapping of polycrystalline structure of biological layers were provided.

It was demonstrated the results of experimental approbation of such method and defined the distributions of Jones-matrix elements of polycrystalline film of urine.

The differentiation of such samples was realized with good and excellent levels of balanced accuracy of differentiation between normal uterus wall tissue and with prolapse.

References

1. Tuchin V., Tissue Optics: Light Scattering Methods and Instruments for Medical Diagnostics, 3rd ed., Vol. PM 254, SPIE Press, Bellingham, Washington 2015.

2. Born M., Wolf E., Principles of Optics, Cambridge Univ. Press 1999.

3. Tuchin V., Wang L., Zimnyakov D., Optical Polarization in Biomedical Applications, New York 2006.

4. Ghosh N., Wood M., Vitkin I., Polarized light assessment of complex turbid media such as biological tissues via Mueller matrix decomposition, in Handbook of Photonics for Biomedical Science, V.V. Tuchin, Ed., CRC Press, Taylor & Francis Group, London 2010, pp. 253–282.

5. Ghosh N., Vitkin I., Tissue polarimetry: concepts, challenges, applications and outlook, J. Biomed. Opt. 16, 110801, 2011.

6. Jacques S., Polarized light imaging of biological tissues, in Handbook of Biomedical Optics, D. Boas, C. Pitris, and N. Ramanujam, Eds., CRC Press, Boca Raton, London, New York, 2011, pp. 649–669.

7. Swami M., Patel H., Gupta P., Conversion of 3 × 3 Mueller matrix to 4 × 4 Mueller matrix for non-depolarizing samples, Opt. Commun. 286(1), 2013, pp. 18–22.

8. Tervo J., Setala T., Friberg A., Degree of coherence for electromagnetic fields, Opt. Express 11, 2003, pp. 1137-1143.

9. Angelsky, O. V., Bekshaev, A. Ya., Maksimyak, P. P., Maksimyak, A. P., Hanson, S. G., Zenkova, C. Yu., “Self-diffraction of continuous laser radiation in a disperse medium with absorbing particles,” Optics Express 21(7), 8922-8938 (2013).

10. Angelsky, O.V., Bekshaev, A. Ya., Maksimyak, P. P., Maksimyak, A. P., Hanson, S.G. ,Zenkova, C. Yu., “Self-action of continuous laser radiation and Pearcey diffraction in a water suspension with light-absorbing particles,” Optics Express 22(3), 2267-2277 (2014).

11. Angelsky, O. V., Bekshaev, A. Ya., Maksimyak, P. P., Maksimyak, A. P., Hanson, S. G., “Measurement of small light absorption in microparticles by means of optically induced rotation,” Optics Express 23(6), 7152-7163 (2015).

12. Polyanskii, V.K., Angelsky, O.V., Polyanskii, P.V., “Scattering-induced spectral changes as a singular optical effect,” Optica Applicata 32 (4), 843-848 (2002).

13. Angelsky, O.V., Besaha, R.N., Mokhun, A.I., Mokhun, I.I., Sopin, M.O., Soskin, M.S., “Singularities in vectoral fields,” Proc. SPIE 3904, 40-54 (1999).

14. Angelsky, O.V., Tomka, Y.Y., Ushenko, A.G., Ushenko, Y.G., Yermolenko, S.B., “2-D tomography of biotissue images in pre-clinic diagnostics of their pre-cancer states,” Proc. SPIE 5972, 158-162 (2005).

15. Angelsky, O.V., Gorky, M.P., Hanson, S.G., Lukin, V.P., Mokhun, I. I., Polyanskii, P.V., Ryabiy, P.A., “Optical correlation algorithm for reconstructing phase skeleton of complex optical fields for solving the phase problem,” Opt. Exp. 22(5), 6186-6193 (2014).

16. Ushenko A., Pishak V., Laser Polarimetry of Biological Tissue: Principles and Applications, Handbook of Coherent-Domain Optical

Methods: Biomedical Diagnostics, Environmental and Material Science, 2004, pp. 93–138.

17. Angelsky O., Ushenko A., Ushenko Yu., Pishak V., Peresunko A., Statistical, Correlation and Topological Approaches in Diagnostics of the Structure and Physiological State of Birefringent Biological Tissues, Handbook of Photonics for Biomedical Science, 2010, pp. 283-322.

18. Ushenko Y., Boychuk T., Bachynsky V., Mincer O., Diagnostics of Structure and Physiological State of Birefringent Biological Tissues: Statistical, Correlation and Topological Approaches in Handbook of Coherent-Domain Optical Methods, ISBN 978-1-4614-5175-4. Springer Science+Business Media New York, 2013, pp. 107-148.

19. Ushenko Yu., Investigation of formation and interrelations of polarization singular structure and Mueller-matrix images of biological tissues and diagnostics of their cancer changes, J. Biomed. Opt. 16 (6), 066006-066006, 2011.

20. Ushenko V., Two-dimensional Mueller matrix phase tomography of self-similarity birefringence structure of biological tissues, Proc. SPIE 8487, Novel Optical Systems Design and Optimization XV, 2012, pp. 84870W.

21. Ushenko Yu., Ushenko V., Dubolazov A., Balanetskaya V., Zabolotna N., Mueller-matrix diagnostics of optical properties of polycrystalline networks of human blood plasma., Optics and Spectroscopy, Volume 112, Issue 6, 2012, pp 884-892.

22. Ushenko Yu., Dubolazov A., Balanetskaya V., Karachevtsev A., Ushenko V., Wavelet-analysis of polarization maps of human blood plasma, Optics and Spectroscopy, Volume 113, Issue 3, 2012, pp 332-343.

23. Ushenko V., Gavrylyak M., Azimuthally invariant Mueller-matrix mapping of biological tissue in differential diagnosis of mechanisms

protein molecules networks anisotropy, Proc. SPIE 8812, Biosensing and Nanomedicine VI, 2013, pp. 88120Y.
24. Ushenko V., Pavlyukovich N., Trifonyuk L., Spatial-Frequency Azimuthally Stable Cartography of Biological Polycrystalline Networks, International Journal of Optics, Volume 2013, 2013, Article ID 683174.
25. Ushenko V., Spatial-frequency polarization phasometry of biological polycrystalline networks, Optical Memory and Neural Networks, Volume 22, Issue 1, 2013, pp. 56-64.
26. Ushenko V., Dubolazov O., Karachevtsev A., Two wavelength Mueller matrix reconstruction of blood plasma films polycrystalline structure in diagnostics of breast cancer, Applied Optics Vol. 53, Issue 10, 2014, pp. B128-B139.
27. Ushenko A., Pashkovskaya N., Dubolazov O., Ushenko Yu., Marchuk Yu., Ushenko V., Mueller matrix images of polycrystalline films of human biological fluids, Romanian reports in physics. 67(4), 2015, pp. 1467-1479.
28. Prysyazhnyuk V., Ushenko Yu., Dubolazov A., Ushenko A., Ushenko V., Polarization-dependent laser autofluorescence of the polycrystalline networks of blood plasma films in the task of liver pathology differentiation, Appl. Opt. 55, 2016, pp. B126-B132.
29. Dubolazov A., Pashkovskaya N., Ushenko Yu., Marchuk Yu., Ushenko V., Novakovskaya O., Birefringence images of polycrystalline films of human urine in early diagnostics of kidney pathology, Appl. Opt. 55, 2016, pp. B85-B90.
30. Ushenko Yu., Koval G., Ushenko A., Dubolazov O., Ushenko V., Novakovskaia O., Mueller-matrix of laser-induced autofluorescence of polycrystalline films of dried peritoneal fluid in diagnostics of endometriosis, J. Biomed. Opt. 21(7), 2016, 071116.
31. Ushenko Yu., Gorskii M., Dubolazov A., Motrich A., Ushenko V.,

Sidor M., Spatial-frequency Fourier polarimetry of the complex degree of mutual anisotropy of linear and circular birefringence in the diagnostics of oncological changes in morphological structure of biological tissues, Quantum Electron,Volume 42(8), 2012.

32. Ushenko V., Complex degree of mutual coherence of biological liquids, Proc. SPIE 8882, ROMOPTO 2012: Tenth Conference on Optics: Micro- to Nanophotonics III, 2013, pp. 88820V.

33. Ushenko V., Gorsky M., Complex degree of mutual anisotropy of linear birefringence and optical activity of biological tissues in diagnostics of prostate cancer, Optics and Spectroscopy, Volume 115, Issue 2, 2013, pp 290-297.

34. Ushenko Yu., Bachynsky V., Vanchulyak O., Dubolazov A., Garazdyuk M., Ushenko V., Jones-matrix mapping of complex degree of mutual anisotropy of birefringent protein networks during the differentiation of myocardium necrotic changes, Appl. Opt. 55, 2016, pp. B113-B119.

35. Tervo J., Setala T., Friberg A., Two-point Stokes parameters: interpretation and properties, Optics Letters 34(20), 2009, pp. 3074-3076.

36. L. Cassidy, "Basic concepts of statistical analysis for surgical research," *Journal of Surgical Research* 128, 199-206 (2005).

37. C. S. Davis, “Statistical methods of the analysis of repeated measurements,” *New York: Springer-Verlag*, 744, (2002).

38. A. Petrie, B. Sabin, “Medical Statistics at a Glance,” *Blackwell Publishing*, 157, (2005).